

Isolation of an Extremely Labile Dihydrogen Complex, $\text{Cr}(\text{CO})_3(\text{PPr}^i)_2(\text{H}_2)$, Containing the Shortest Ligated H–H Bond

Gregory J. Kubas,^{*,†} Janet E. Nelson,[†] Jeffrey C. Bryan,[†] Juergen Eckert,[†] Linda Wisniewski,[‡] and Kurt Zilm[‡]

CST-3 and LANSCE Groups, MS-C346, Los Alamos National Laboratory, Los Alamos, New Mexico 87545, and Department of Chemistry, Yale University, New Haven, Connecticut 06520

Received December 27, 1993[⊙]

First-row members of the group 6 series of transition metal dihydrogen complexes $\text{Cr}(\text{CO})_3(\text{PR}_3)_2(\eta^2\text{-H}_2)$ ($\text{R} = \text{Cy}, \text{Pr}^i$) have been synthesized and examined by X-ray crystallography and NMR, infrared, and inelastic neutron scattering spectroscopies. The complexes completely dissociate H_2 in solution to give $\text{Cr}(\text{CO})_3(\text{PR}_3)_2$, which contains an agostic C–H interaction. An X-ray structure of $\text{Cr}(\text{CO})_3(\text{PPr}^i)_2(\text{H}_2)$ showed a side-bonded dihydrogen ligand with H–H = 0.67(5) Å, and proton NMR of the HD isotopomer showed a $J(\text{HD})$ value of 35 Hz. Solid-state ^1H NMR spectroscopy of the PCy_3 complex indicated that the H–H separation is 0.85(1) Å, which is believed to be a more precise and accurate measure of this key parameter. The barrier to rotation of the $\eta^2\text{-H}_2$ has been recalculated to be 1.17(10) kcal/mol, as compared with 1.32(10) and 1.9(1) kcal/mol for the Mo and W analogues, based on H–H distances from solid-state NMR. Correlations of properties of the group 6 species indicate that the $\text{H}_2 \rightarrow \text{M} \sigma$ -bonding strength appears to increase as $\text{Mo} < \text{Cr} \sim \text{W}$ but that $d\pi \rightarrow \text{H}_2 \sigma^*$ back-bonding increases down the group. It might be generally concluded that back-bonding is more of a factor than σ -bonding in influencing stability, H–H distance, and possibly overall bond strengths. Crystallographic data: space group $P2_1/c$, $a = 13.457(3)$ Å, $b = 11.493(3)$ Å, $c = 16.639(4)$ Å, $\beta = 102.25(2)^\circ$, $Z = 4$, $R = 3.32\%$.

Introduction

In order to complete the group 6 series of dihydrogen complexes $\text{M}(\text{CO})_3(\text{PR}_3)_2(\text{H}_2)$ ¹ and study periodic trends in structure/reactivity, we have sought to prepare the first-row chromium analogues. Unlike the case for the Mo and W congeners, the reaction of $\text{Cr}(\text{CO})_3(\text{cycloheptatriene})$ with PCy_3 failed to give either $\text{Cr}(\text{CO})_3(\text{PCy}_3)_2(\text{H}_2)$ or the 16- e^- precursor $\text{Cr}(\text{CO})_3(\text{PCy}_3)_2$. Hoff² found that reaction of $\text{Cr}(\text{CO})_3(\text{naphthalene})$ with 2 equiv of PCy_3 in THF under argon did yield $\text{Cr}(\text{CO})_3(\text{PCy}_3)_2$ and rationalized that displacement occurs because the arene is less tightly bound than the triene by nearly 13 kcal/mol.³ Solutions of $\text{Cr}(\text{CO})_3(\text{PCy}_3)_2$ coordinated H_2 , but only under high pressure (300 psi for 100% complexation).² As reported in a recent communication,⁴ we found that under proper conditions $\text{Cr}(\text{CO})_3(\text{PCy}_3)_2(\text{H}_2)$ could be crystallized from solution as a stable solid under 1 atm of H_2 . Both thermodynamic and steric factors play crucial roles in the synthetic strategies and reactivities of these systems. As for $\text{W}(\text{CO})_3(\text{PR}_3)_2(\text{H}_2)$, $\text{Cr}(\text{CO})_3(\text{PR}_3)_2(\text{H}_2)$ could be synthesized only for $\text{R} = \text{Cy}$ and Pr^i , despite numerous variations of the R groups in the synthetic procedure. Details of this work, including the synthesis, characterization, and X-ray structure of the PPr^i analogue, will be described here. $\text{Cr}(\text{CO})_3(\text{PPr}^i)_2(\text{H}_2)$ represents to date the most unstable isolatable H_2 complex⁵ and contains the shortest H–H

distance found for metal-bound dihydrogen, as determined by solid-state ^1H NMR⁶ and X-ray crystallographic methods.

Experimental Section

Reactions were carried out under argon and/or H_2 atmospheres using Schlenk techniques or in a helium-filled inert-atmosphere glovebox. Solvents distilled from Na/K alloy and high-purity argon and/or H_2 were generally used in the syntheses and NMR spectroscopy. Phosphines were purchased from Strem Chemical. $\text{Cr}(\text{CO})_3(\text{naphthalene})$ and $\text{Cr}(\text{CO})_3(\text{PCy}_3)_2$ were either obtained as gifts from Carl Hoff of the University of Miami or synthesized by published procedures.² FT-IR and ^1H NMR spectra were recorded on Bio-Rad FTS-40 and Bruker AM-200 instruments. ^{31}P NMR utilized a 250-MHz IBM instrument and H_3PO_4 reference. Elemental analyses were performed by Galbraith Laboratories, Inc., Knoxville, TN.

High-Pressure Syntheses of $\text{Cr}(\text{CO})_3(\text{PCy}_3)_2(\text{H}_2)$ from $\text{Cr}(\text{CO})_3(\text{PCy}_3)_2$. A small sample of $\text{Cr}(\text{CO})_3(\text{PCy}_3)_2$ was dissolved in 2 mL of toluene in a Fisher-Porter heavy-wall glass reactor tube and pressurized to 70 psi of H_2 atmosphere. The deep ink-blue solution immediately became tan-yellow, and a yellow solid, presumably $\text{Cr}(\text{CO})_3(\text{PCy}_3)_2(\text{H}_2)$, precipitated in ~ 5 min. Reducing the pressure to 40 psi gave a small amount of darkening of solution color, and at 30 psi a gray-blue color appeared. At atmospheric pressure, the solution returned to the original blue color, but some yellow solid remained.

A second, preparative-scale reaction was carried out using a solution of $\text{Cr}(\text{CO})_3(\text{PCy}_3)_2$ prepared in situ. A solution of 0.980 g (3.71 mmol) of $\text{Cr}(\text{CO})_3(\text{naphthalene})$ and 2.25 g (8.02 mmol) of PCy_3 in 18 mL of THF was reacted under argon for 2.5 d *without stirring*. The resulting deep-blue solution, which probably was supersaturated, was transferred to the reactor tube and pressurized to 60 psi of H_2 . A yellow precipitate began to form near the surface within minutes, and larger orange-yellow crystals slowly formed over the next 3 d. The latter were isolated by decantation in a glovebag. As soon as the pressure was released, the mother liquor evolved H_2 and became blue. The crystalline mass of $\text{Cr}(\text{CO})_3(\text{PCy}_3)_2(\text{H}_2)$ was washed in the reaction tube with 1:1 hexane-toluene and dried by several brief alternate exposures to vacuum and H_2

[†] Los Alamos National Laboratory.

[‡] Yale University.

[⊙] Abstract published in *Advance ACS Abstracts*, May 15, 1994.

- (a) Kubas, G. J.; Ryan, R. R.; Swanson, B. I.; Vergamini, P. J.; Wasserman, H. J. *J. Am. Chem. Soc.* **1984**, *106*, 451. (b) Kubas, G. J.; Unkefer, C. J.; Swanson, B. I.; Fukushima, E. *J. Am. Chem. Soc.* **1986**, *108*, 7000.
- (a) Gonzalez, A. A.; Mukerjee, S. L.; Chou, S.-J.; Zhang, K.; Hoff, C. D. *J. Am. Chem. Soc.* **1988**, *110*, 4419. (b) Millar, J. M.; Kastrop, R. V.; Melchior, M. T.; Horvath, I. T.; Hoff, C. D.; Crabtree, R. H. *J. Am. Chem. Soc.* **1990**, *112*, 9643. (c) Zhang, K.; Gonzalez, A. A.; Mukerjee, S. L.; Chou, S.-J.; Hoff, C. D.; Kubat-Martin, K. A.; Barnhart, D.; Kubas, G. J. *J. Am. Chem. Soc.* **1991**, *113*, 9170.
- Mukerjee, S. L.; Lang, R. F.; Ju, T.; Kiss, G.; Hoff, C. D. *Inorg. Chem.* **1992**, *31*, 4885.
- Eckert, J.; Kubas, G. J.; White, R. P. *Inorg. Chem.* **1992**, *31*, 1550.

- (5) Reviews of H_2 complexes: (a) Kubas, G. J. *Acc. Chem. Res.* **1988**, *21*, 120. (b) Crabtree, R. H. *Acc. Chem. Res.* **1990**, *23*, 95. (c) Jessop, P. G.; Morris, R. H. *Coord. Chem. Rev.* **1992**, *121*, 155. (d) Heinekey, D. M.; Oldham, W. J., Jr. *Chem. Rev.* **1993**, *93*, 913. (e) Crabtree, R. H. *Angew. Chem., Int. Ed. Engl.* **1993**, *32*, 789.
- (6) Zilm, K. W.; Millar, J. M. *Adv. Magn. Opt. Reson.* **1990**, *15*, 163.

Table 1. Crystallographic Data

chem formula	$C_{21}H_{44}CrO_3P_2$	space group	$P2_1/c$
$a, \text{\AA}$	13.457(3)	$T, ^\circ C$	-70
$b, \text{\AA}$	11.493(3)	$\lambda, \text{\AA}$	0.710 73
$c, \text{\AA}$	16.639(4)	$\rho_{\text{calc}}, \text{g}\cdot\text{cm}^{-3}$	1.211
β, deg	102.25(2)	μ, cm^{-1}	5.99
$V, \text{\AA}^3$	2514.8(16)	R^a	0.0332
Z	4	R_w^b	0.0427 ^c
f_w	458.4		

$$^a R = \sum(|F_o| - |F_c|) / \sum |F_o|, \quad ^b R_w = [\sum w(|F_o| - |F_c|)^2 / \sum w |F_o|^2]^{1/2}, \quad ^c w = [\sigma^2(F_o) + 0.0003 F_o^{2+}]^{-1}.$$

(yield, 2.0 g, 77%). The crystals were air-stable for short periods but became green-tinged on the surface within 2 h.

Synthesis of $Cr(CO)_3(PCy_3)_2(H_2)$ Directly from $Cr(CO)_3(\text{naphthalene})$ at Atmospheric Pressure. A mixture of 0.980 g (3.71 mmol) of $Cr(CO)_3(\text{naphthalene})$ and 2.25 g (8.02 mmol) of PCy_3 in 18 mL of THF was magnetically stirred under an H_2 atmosphere. After about 3 h a yellow precipitate began to form, which was collected on a frit after further reaction for 20 h. The resulting bright yellow powder was thoroughly washed with hexane (80 mL) to remove any naphthalene coproduct and dried under a stream of H_2 . The yield of $Cr(CO)_3(PCy_3)_2(H_2)$ was 2.10 g (81%). The D_2 complex was prepared identically. Nujol mull IR samples were prepared in glovebags containing argon-hydrogen mixtures.

Synthesis of $Cr(CO)_3(PPr^i_3)_2$. A 1.0-g sample of $Cr(CO)_3(\text{naphthalene})$ was dissolved in 5 mL of THF, and 1.3 g of PPr^i_3 was added. The yellow solution turned red and then deep purple over the course of 6 h. This solution decomposes easily in solution, presumably via disproportionation to $Cr(CO)_4(PPr^i_3)_2$.

Synthesis of $Cr(CO)_3(PPr^i_3)_2(H_2)$. The THF solution of the above $Cr(CO)_3(PPr^i_3)_2$ complex was charged with ca. 1 atm of H_2 at $-78^\circ C$. Hexanes were added to precipitate a yellow powder. The solution was filtered cold, and the solid was dried with an H_2 stream. There was some loss of H_2 , even under a hydrogen atmosphere, giving a green appearance to the surface of the solid because of formation of blue $Cr(CO)_3(PPr^i_3)_2$. The H_2 complex was recrystallized from diethyl ether to remove traces of naphthalene (yield: 0.6 g, 40%). The HD congener was prepared for solution NMR studies by substituting HD gas (Matheson) for H_2 .

X-ray Crystal Structure of $Cr(CO)_3(PPr^i_3)_2(H_2)$. Large yellow crystals were obtained by cooling a saturated Et_2O solution of $Cr(CO)_3(PPr^i_3)_2(H_2)$ to $-20^\circ C$. Crystals were examined under a H_2 -argon atmosphere, and a large rod-shaped crystal was selected, cleaved to smaller size, mounted on a glass fiber, and placed under the cold stream (N_2) of the diffractometer. Preliminary photographic examination and data collection were performed on a Siemens R3m/V diffractometer at $-70^\circ C$. Cell constants and an orientation matrix were obtained by least-squares refinement, using the setting angles of 30 reflections in the range $8 < 2\theta < 30^\circ$. Good crystal quality was also suggested by measuring ω scans of several intense reflections and by examining axial photographs. Intensity data were obtained using θ - 2θ scans. The scan rate was varied between 3.66 and 14.65 $^\circ/\text{min}$ in ω . A total of 12 277 reflections ($\pm h, \pm k, \pm l$) were collected. The unit cell and systematic absences suggested the space group $P2_1/c$ (No. 14). The data were scaled for linear decay (minimum and maximum corrections were 0.997 and 1.10, respectively), and a semiempirical absorption correction based on the average relative intensity curve of azimuthal scan data was applied. The data were averaged over $2/m$ symmetry ($R_{\text{int}} = 3.9\%$).

The chromium and phosphorus atom positions were revealed by direct methods. All remaining atoms were located in succeeding difference Fourier maps, and all non-hydrogen atoms were refined anisotropically. Atoms H1 and H2 were refined isotropically. All other hydrogen atoms were added to the structure factor calculations without refinement. Only the 4599 independent reflections with $F > 4\sigma_F$ were used in the refinements. The final cycle of refinement with 252 parameters converged (largest parameter shift was 0.007σ) with $R = 0.033$ and $R_w = 0.043$ and a goodness-of-fit $S = 1.5$. The highest peak in the final difference Fourier map had a height of $0.32 e/\text{\AA}^3$ and is associated with a phosphorus atom. All calculations were performed using SHELXTL PLUS programs provided by Siemens Analytical. A structure determination summary is given in Table 1, positional and equivalent isotropic thermal parameters of the non-hydrogen atoms are listed in Table 2, and bond lengths and bond angles are given in Tables 3 and 4. A complete structure summary, anisotropic thermal parameters, and hydrogen atom coordinates are given in the supplementary material.

Table 2. Atomic Coordinates ($\times 10^4$) and Equivalent Isotropic Displacement Coefficients ($\text{\AA}^2 \times 10^3$)

	x	y	z	$U(\text{eq})^a$
Cr	7592(1)	309(1)	3700(1)	23(1)
H(1)	7391(24)	-710(30)	4471(20)	76(11)
H(2)	7622(28)	-231(33)	4657(22)	97(13)
P(1)	7447(1)	1982(1)	4500(1)	22(1)
P(2)	7662(1)	-1536(1)	3071(1)	26(1)
C(1)	6190(2)	351(2)	3283(1)	37(1)
O(1)	5332(1)	419(2)	2988(1)	64(1)
C(2)	9015(2)	374(2)	4012(1)	33(1)
O(2)	9891(1)	479(2)	4143(1)	55(1)
C(3)	7766(2)	1143(2)	2814(1)	31(1)
O(3)	7912(1)	1688(1)	2257(1)	47(1)
C(10)	7133(1)	1691(2)	5522(1)	28(1)
C(11)	6102(2)	1069(2)	5439(1)	44(1)
C(12)	7969(2)	1001(2)	6101(1)	37(1)
C(13)	8647(1)	2851(2)	4808(1)	29(1)
C(14)	9035(2)	3336(2)	4082(1)	51(1)
C(15)	8695(2)	3792(2)	5460(1)	40(1)
C(16)	6392(2)	3002(2)	4038(1)	35(1)
C(17)	6474(2)	3492(3)	3217(2)	76(1)
C(18)	6150(2)	3971(2)	4589(2)	67(1)
C(20)	7370(2)	-2790(2)	3695(1)	42(1)
C(21)	8171(2)	-2927(2)	4496(2)	56(1)
C(22)	6294(2)	-2706(2)	3860(2)	57(1)
C(23)	8950(2)	-1940(2)	2907(1)	34(1)
C(24)	9325(2)	-1109(2)	2322(1)	47(1)
C(25)	9141(2)	-3200(2)	2677(2)	53(1)
C(26)	6719(2)	-1784(2)	2086(1)	35(1)
C(27)	6718(2)	-2968(2)	1672(2)	54(1)
C(28)	6726(2)	-830(2)	1451(1)	53(1)

^a Equivalent isotropic U defined as one-third of the trace of the orthogonalized U_{ij} tensor.

Table 3. Selected Bond Lengths (\AA) and Angles (deg) for $Cr(CO)_3(PPr^i_3)_2(H_2)$ Not Given in Table 4

C(1)-O(1)	1.157(3)	C(2)-O(2)	1.159(3)
C(3)-O(3)	1.169(3)		
H(1)-Cr-P(1)	94.9(11)	H(2)-Cr-P(1)	76.1(13)
H(1)-Cr-P(2)	76.1(11)	H(2)-Cr-P(2)	95.3(13)
H(1)-Cr-C(1)	89.4(10)	H(2)-Cr-C(1)	100.3(12)
P(2)-Cr-C(1)	89.5(1)	H(1)-Cr-C(2)	97.4(10)
H(2)-Cr-C(2)	86.3(12)	P(2)-Cr-C(2)	91.4(1)
H(2)-Cr-C(3)	166.2(12)	P(2)-Cr-C(3)	95.1(1)
Cr-H(1)-H(2)	71(4)	Cr-H(2)-H(1)	87(4)
Cr-C(1)-O(1)	176.0(2)	Cr-C(2)-O(2)	173.8(2)
Cr-C(3)-O(3)	177.6(2)		

Table 4. Comparison of Selected Distances and Angles for $M(CO)_3(PPr^i_3)_2(H_2)$ ($M = Cr, W$)

	distances, \AA		distances, \AA		
	Cr	W	Cr	W	
M-P(1)	2.370(1)	2.487(4)	M-C(3)	1.815(2)	1.977(16)
M-P(2)	2.375(1)	2.503(4)	M-H(1)	1.80(3)	2.12(12)
M-C(1)	1.868(2)	2.036(17)	M-H(1)	1.70(4)	1.76(13)
M-C(2)	1.876(2)	2.025(19)	H(1)-H(2)	0.67(5)	0.75(16)
		angles, deg		angles, deg	
		Cr	W	Cr	W
P(1)-M-P(2)	170.9(1)	178.3(1)	P(1)-M-C(3)	93.9(1)	90.1(4)
C(1)-M-C(2)	173.2(1)	176.0(5)	C(1)-M-C(3)	88.8(1)	91.7(6)
C(3)-M-H(1)	171(1)	171(3)	C(2)-M-C(3)	84.4(1)	92.0(6)
P(1)-M-C(1)	89.5(1)	90.1(4)	H(1)-M-H(2)	22.0(16)	20(5)
P(1)-M-C(2)	90.8(1)	88.0(4)			

Solid-State NMR Studies. Solid-state 1H NMR spectra of $Cr(CO)_3(PCy_3)_2(\eta^2-H_2)$ were obtained at 7.05 T with a homebuilt spectrometer. A powder sample was prepared as stated above and sealed under hydrogen gas. Spectra were obtained over the range of 100 K to room temperature. The pulse sequence consisted of a weak pulse followed by a dipolar echo.⁶ The dipolar echo eliminated pulse breakthrough, which can obscure the first few points of the free induction decay. The soft pulse selectively attenuates the hydrogen signal from the phosphine ligands so that the dihydrogen contribution can be seen more clearly. The resulting room-

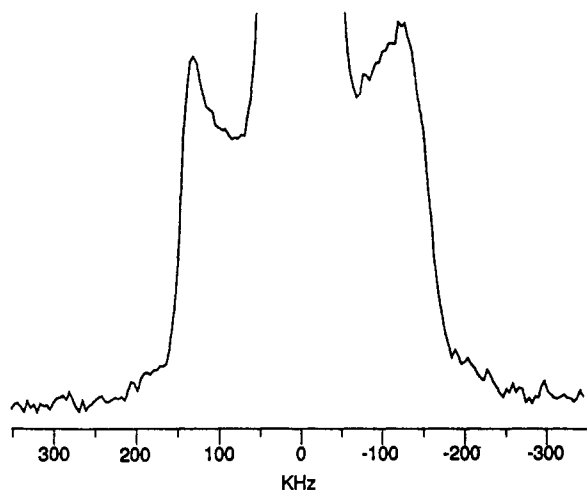
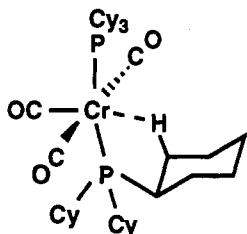


Figure 1. Solid state NMR spectrum of a $\text{Cr}(\text{CO})_3(\text{PCy}_3)_2(\eta^2\text{-H}_2)$ powder sample at room temperature and 7.05 T as described in the text.

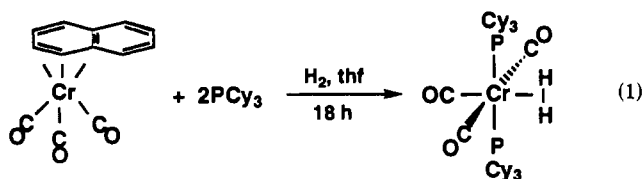
temperature spectrum is shown in Figure 1. The truncated central line is the remaining contribution from the imperfectly suppressed phosphine peak. The modified Pake doublet flanking this peak corresponds to a nonclassical dihydrogen ligand.

Results and Discussion

Synthesis and Properties of $\text{Cr}(\text{CO})_3(\text{PR}_3)_2(\text{H}_2)$. The X-ray structure^{2c} of the unsaturated complex $\text{Cr}(\text{CO})_3(\text{PCy}_3)_2$ showed an agostic interaction ($\text{Cr}\cdots\text{H} = 2.240(1) \text{ \AA}$) identical to that first found in the tungsten analogue.⁷



This deep-blue species did not noticeably discolor in air for at least 30 min even when finely powdered and in general coordinated small molecules such as N_2 more weakly than the Mo and W congeners, probably because of more steric crowding.² When exposed to high pressures of hydrogen (ca 300 psi), powdered $\text{Cr}(\text{CO})_3(\text{PCy}_3)_2$ became yellow, indicative of H_2 adduct formation similar to the solution-phase reaction.² The hydrogen readily dissociated in vacuo or under argon. Unexpectedly, finely powdered $\text{Cr}(\text{CO})_3(\text{PCy}_3)_2$ turned yellow on the surface even when exposed to hydrogen at atmospheric pressure, suggesting that it might be possible to crystallize the H_2 complex from solution as a stable solid under proper conditions. Indeed $\text{Cr}(\text{CO})_3(\text{PR}_3)_2(\text{H}_2)$ ($\text{R} = \text{Cy}, \text{Pr}^i$) can be directly synthesized and isolated (eq 1) identically to the Mo and W analogues,⁸ except substituting



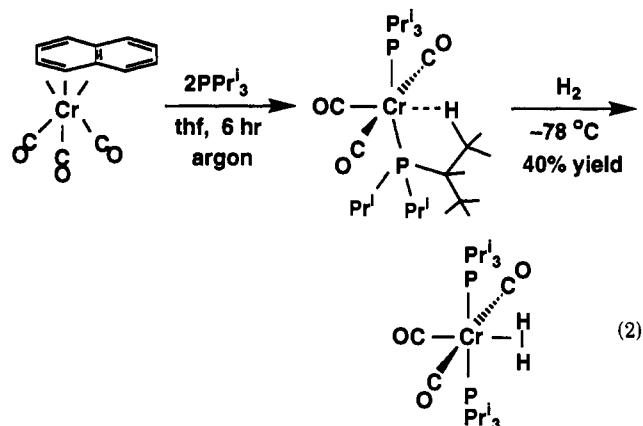
$\text{Cr}(\text{CO})_3(\eta^6\text{-naphthalene})$ for $\text{M}(\text{CO})_3(\eta^6\text{-cycloheptatriene})$ and

(7) Wasserman, H. J.; Kubas, G. J.; Ryan, R. R. *J. Am. Chem. Soc.* **1986**, *108*, 2294.

(8) Kubas, G. J. *Inorg. Synth.* **1990**, *27*, 1.

using THF as solvent rather than toluene (which forms $\text{Cr}(\text{CO})_3(\eta^6\text{-toluene})$ containing tightly-bound toluene).

$\text{Cr}(\text{CO})_3(\text{PCy}_3)_2(\text{H}_2)$ precipitated as bright yellow microcrystals in 81% yield, demonstrating that H_2 is a better ligand than THF, probably for steric reasons. The solid PCy_3 complex is stable under partial pressures of H_2 . Unlike the latter, the PPr^i_3 species must be prepared at low temperature via a two-step procedure (eq 2). $\text{Cr}(\text{CO})_3(\text{PPr}^i_3)_2(\text{H}_2)$ dissociates H_2 even when



kept under 1 atm of H_2 during filtration from solution and drying at room temperature. The surfaces of the yellow crystals that form at low temperature immediately turn green, presumably because of admixture with blue $\text{Cr}(\text{CO})_3(\text{PPr}^i_3)_2$. Further H_2 loss slowly gives a color change to deep blue even when the complex is kept in a sealed tube under H_2 . $\text{Cr}(\text{CO})_3(\text{PPr}^i_3)_2(\text{H}_2)$ thus appears to be the most unstable⁹ dihydrogen complex among those that can be isolated as a solid at room temperature (many low-temperature stable H_2 complexes are known,^{5d} generally prepared by photolytic substitution of CO in noble-gas media or by protonation of hydrides). In order to collect crystallographic data on this complex (see below), a large single crystal was rapidly cleaved to smaller size and immediately placed in the cold stream of the diffractometer. At 203 K the complex survived data collection for several days without significant decomposition. Attempts to prepare more stable analogues with other phosphines (e.g. PPh_3 and PBu^t_3) yielded only red oily materials that were not characterized, as previously found for reactions of these phosphines with $\text{W}(\text{CO})_3(\eta^6\text{-cycloheptatriene})$ in toluene under either H_2 or argon.

There are several anomalies in both the formation and relative stabilities of the Cr complexes in solid versus solution phases. Because solutions of $\text{Cr}(\text{CO})_3(\text{PCy}_3)_2$ do not bind H_2 at 1 atm, it is difficult to understand why the H_2 complex precipitates in eq 1 in favor of $\text{Cr}(\text{CO})_3(\text{PCy}_3)_2$, the logical intermediate. The low solubility of the H_2 complex might be a factor, although this alone does not explain why concentrated solutions of $\text{Cr}(\text{CO})_3(\text{PCy}_3)_2$ do not precipitate the H_2 complex. Furthermore, when solid $\text{Cr}(\text{CO})_3(\text{PCy}_3)_2(\text{H}_2)$ is placed into toluene, *instantaneous complete dissociation of H_2 occurs, even under an H_2 atmosphere*, to give a deep blue-purple solution of $\text{Cr}(\text{CO})_3(\text{PCy}_3)_2$. The overall behavior suggests that in eq 1 the H_2 somehow becomes "trapped" in the solid phase (possibly due to supersaturation effects) and is less able to escape out of the crystal lattice than in the solution phase. This is reasonable in that the H_2 is not merely leaving the coordination site in these complexes; the whole molecule must rearrange to give the agostic interaction in the structure of $\text{Cr}(\text{CO})_3(\text{PCy}_3)_2$. When dissolved in a solvent such as toluene, $\text{Cr}(\text{CO})_3(\text{PCy}_3)_2(\text{H}_2)$ would be more flexible in its ability to move a cyclohexyl ring into position to displace the H_2 .

(9) In terms of reversible H_2 dissociation, iridium-dihydrogen complexes are also very labile: Mediatl, M.; Tachibana, G. N.; Jensen, C. M. *Inorg. Chem.* **1990**, *29*, 3; **1992**, *31*, 1827.

It is also conceivable that the solvent assists this process by mass action effects, i.e. initial displacement of the H_2 to form equilibrium amounts of a very weak solvento complex which then rapidly goes to the agostic complex. Solvent competition, even from toluene (which cannot be an η^6 ligand here for steric reasons), may explain why large H_2 pressures must be used to force formation of the H_2 complex from $Cr(CO)_3(PCy_3)_2$ in solution.

Counterintuitively, the relative solution-solid-state stabilities of $Cr(CO)_3(PPr^i_3)_2(H_2)$ appear to be the reverse of those of the PCy_3 congener. The former easily loses H_2 in the solid state even under H_2 to give $Cr(CO)_3(PPr^i_3)_2$ yet can be dissolved in and recrystallized from Et_2O without significant H_2 loss, although low temperatures are necessary. Thermodynamic measurements showed that for the tungsten- H_2 derivatives the PPr^i_3 species coordinated H_2 slightly more strongly ($\Delta\Delta H = 0.8$ kcal/mol) than the PCy_3 congener in toluene solution.^{10e} This correlates with the higher stability of $Cr(CO)_3(PPr^i_3)_2(H_2)$ over $Cr(CO)_3(PCy_3)_2(H_2)$ in solution, but the reversed solid-state stabilities are puzzling. Relative energies of the agostic interaction could be important here. We have been unable to directly measure these, but it is notable that $Cr(CO)_3(PR_3)_2$ is more unstable in solution toward disproportionation to $Cr(CO)_4(PR_3)_2$ than $Cr(CO)_3(PCy_3)_2$ and could not be isolated. It must additionally be kept in mind that the energies¹⁰ of the metal σ -bond interactions in these complexes are so low (~ 10 – 15 kcal/mol) that entropic factors^{10a} can reverse relative stabilities. Indeed N_2 is more weakly bound than H_2 for the chromium complexes whereas the opposite is true for $M = Mo, W$.

Solution and Solid-State NMR Studies. The 1H NMR spectrum of $Cr(CO)_3(PPr^i_3)_2(H_2)$ in $THF-d_8$ shows a single broad (100 Hz at half-height) resonance due to coordinated H_2 at $\delta -7.65$ (246 K). Unequivocal evidence for an H_2 ligand is provided by the value of $J(HD)$ in $Cr(CO)_3(PPr^i_3)_2(HD)$, which was measured to be 35 Hz in the 1H NMR, slightly higher than that for the W congener (33.5 Hz). Also the value of T_1 was measured to be 6 ms in $THF-d_8$ at 250 MHz. Although a minimum value could not be determined, this value is clearly low enough to indicate dihydrogen binding.^{5b} It should be recalled that the H–H bond cleaves in solution to give an equilibrium amount of dihydride tautomer for $W(CO)_3(PR_3)_2(H_2)$.^{5a} However there was no evidence for this in the Cr system, which correlates with the expected lower degree of activation of the H–H bond owing to the diminished ability of chromium to back-bond to $H_2 \sigma^*$ compared to tungsten.

A lower degree of back-bonding also corresponds with the high lability of H_2 and the higher value of $J(HD)$ compared to those of the W congener. This situation is similar to that for labile $[RuH(H_2)(dppe)_2]^+$ which has $J(HD) = 32$ Hz compared to 30 Hz for the nonlabile Fe analogue (in this particular system the first-row group 8 metal was surprisingly found to be a better back-bonder than the second-row metal).^{5c}

The line shape of the solid-state 1H NMR spectrum (Figure 1) of $Cr(CO)_3(PCy_3)_2(H_2)$ is characterized by a modified Pake pattern. Solid-state NMR spectra are dominated by dipolar interactions, which depend upon the orientation of the dipolar vector within the magnetic field. If the dihydrogen were stationary in this complex, it would yield a typical Pake doublet consisting of two distinct dipolar splittings. Librational motion of the H_2 rotor about its coordination axis alters the orientation of the dipolar vector and hence distorts the experimental line shape. The motionally averaged dipolar tensor in this case is traceless and

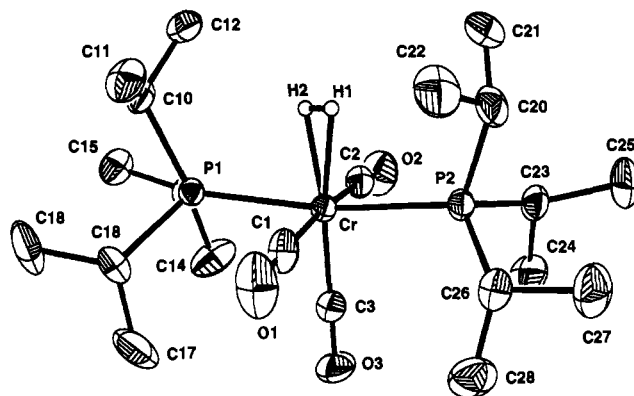


Figure 2. ORTEP (50% probability ellipsoids) drawing of $Cr(CO)_3(PPr^i_3)_2(H_2)$. The atoms of the dihydrogen ligand were refined isotropically and are represented as spheres.

characterized by three distinct splittings.⁶ In the spectrum of Figure 1, the outermost, low-intensity splitting (called the “wings”) and the innermost, high-intensity splitting (“horns”) are apparent. These depend upon the amplitude of the librational motion and therefore are temperature dependent. Computer simulations of the temperature dependence of the line shape suggest that the rotational potential energy function consists of a 2-fold potential with a significant 4-fold contribution. The apparent loss of intensity in the wings is most likely due to anisotropic relaxation effects, which are typical in wide-line NMR spectra of deuterium powders.¹¹ The location of the middle splitting (“shoulders”) is determined by assuming a traceless dipolar tensor. It is not visibly distinguishable in the spectrum shown because it is close in value to the horns. The shoulders measured 281 ± 1 kHz, and, unlike the other two splittings, are temperature independent. The reason is apparent if we consider the motion of the dihydrogen rotor confined to a plane perpendicular to the Cr– H_2 axis. When the rotation axis is aligned with the applied magnetic field, the dipolar splitting is the same regardless of the amplitude of the motion. This splitting is equal to three-halves of the dipolar coupling constant, which in turn is inversely proportional to the cube of the internuclear distance. The measured shoulder width thus corresponds to a dihydrogen bond length of 0.862 Å. NMR-determined values typically overestimate such bond lengths by 0.01 Å, so the actual internuclear distance is more likely 0.85 ± 0.01 Å. This is the shortest ever reported for solid-state NMR, as is reflected by the unusually wide Pake pattern observed for this compound.

X-ray Structure of $Cr(CO)_3(PPr^i_3)_2(H_2)$. Comparison of H–H Distances Determined by Diffraction and Solid State NMR Methods. Large single crystals of $Cr(CO)_3(PPr^i_3)_2(H_2)$ grew in a 10-mm NMR tube under H_2 and were isolated, cleaved to smaller size, and mounted in a nitrogen cold stream before significant decomposition (N_2 does not displace H_2 here). The X-ray structure (Figure 2) was very similar to that for the tungsten analogue,^{1a} except for shorter M–ligand distances and lower standard deviations (Table 4 compares distances and angles for $M = Cr, W$). All hydrogens were located, and the H–H ligand distance was determined to be 0.67(5) Å, which is nominally shorter than the distance in free hydrogen, 0.74 Å. Clearly, this is unreasonable, reflecting the difficulty of determining H–H distances by X-ray diffraction. Because hydrogen has no core electrons (only two bonding electrons), erroneously short H–H distances may result, as here. A much better measure is given by solid state NMR studies, as discussed above, which provide a more direct determination of internuclear H–H separation.

(10) (a) Gonzalez, A. A.; Zhang, K.; Nolan, S. P.; de la Vega, R. L.; Mukerjee, S. L.; Hoff, C. D.; Kubas, G. J. *Organometallics* 1988, 7, 2429. (b) Gonzalez, A. A.; Hoff, C. D. *Inorg. Chem.* 1989, 28, 4295. (c) Zhang, K.; Gonzalez, A. A.; Hoff, C. D. *J. Am. Chem. Soc.* 1989, 111, 3627. (d) Gonzalez, A. A.; Zhang, K.; Mukerjee, S. L.; Hoff, C. D.; Khalsa, G. R. K.; Kubas, G. J. *ACS Symp. Ser.* 1990, 428, 133. (e) Kubas, G. J.; Burns, C. J.; Khalsa, G. R. K.; Van Der Sluis, L. S.; Kiss, G.; Hoff, C. D. *Organometallics* 1992, 11, 3390.

(11) See, for example: (a) Wendoloski, J. J.; Gardner, K. H.; Hirschinger, J.; Miura, H.; English, A. D. *Science* 1990, 247, 431. (b) Hirschinger, J.; English, A. D. *J. Magn. Reson.* 1989, 85, 542.

Table 5. H–H Distances Determined by Diffraction Methods versus Solid-State Proton NMR

complex	H–H dist, Å			J_{HD} , Hz	ref ^a
	X-ray	neutron	NMR		
Cr(CO) ₃ (PPr ₃) ₂ (H ₂)	0.67(5)			35	this paper
Cr(CO) ₃ (PCy ₃) ₂ (H ₂)			0.85(1)		this paper
Mo(CO) ₃ (PCy ₃) ₂ (H ₂)			0.87(1)	6	6
Mo(CO)(dppe) ₂ (H ₂) ^b		0.736(10)	0.88(1)	34	12, 6
		[0.80–0.85] ^c			
W(CO) ₃ (PPr ₃) ₂ (H ₂)	0.75(16)	0.82(1)	0.89(1)	33.5	1a, 5a, 6
W(CO) ₃ (PCy ₃) ₂ (H ₂)			0.89(1)		6
[FeH(H ₂)(dppe) ₂] ⁺	0.87(3)	0.816(16)	0.90(1)	32	24, 25, 6
[CpRu(dppm)(H ₂)] ⁺ ^d	1.01			21.9	27, 28
[CpRu(dmpe)(H ₂)] ⁺ ^e			1.02(1)	22	6, 29

^a In respective orders for the X-ray, neutron, NMR, and J_{HD} measurements. ^b dppe = 1,2-bis(diphenylphosphino)ethane. ^c The distance corrected for the effects of hydrogen librational motion. ^d dppm = bis(diphenylphosphino)methane. ^e dmpe = 1,2-bis(dimethylphosphino)ethane.

The NMR distance is 0.85 Å for the Cr–PCy₃ analogue (the differences in phosphine should not be a significant factor), which is also the shortest H–H ligand distance measured by this technique. This is 0.18 Å longer than the X-ray distance, which further illustrates the disconcerting problem of accurate determination of the key structural parameter in H₂ activation, the H–H bond length.

Table 5 compares X-ray, neutron, and solid-state NMR distances for the H–H bonds in the dihydrogen complexes for which NMR distances are available. In most cases, the NMR distance is 0.06–0.08 Å longer than even the neutron diffraction value, presumably because of the highly dynamic nature of the dihydrogen ligand. For example, rotational–librational motion of the H₂ ligand occurs at temperatures as low as 12 K in *trans*-Mo(CO)(H₂)(dppe)₂ because of the extremely low barrier to rotation, ca. 0.5 kcal/mol, brought about by the symmetric ligand disposition *cis* to the H₂.¹² Significant foreshortening of the H–H distance results: 0.736(10) Å is observed by standard refinement of the neutron diffraction data, which is slightly shorter than that in free H₂. Application of a Trueblood THMA11 correction for motion gave a higher value in the range 0.80–0.85 Å.¹² Thus even neutron data are subject to considerable uncertainty, and the corrected neutron value is still below the NMR value, 0.88 Å, which should be relatively insensitive to M–H₂ rotation. More studies and better data analysis methods will be needed to resolve this general problem.

Table 5 does show consistent trends, and the J_{HD} values track nicely with the H–H distances. The H–H distances increase from Cr to Mo to W, in harmony with the known stabilities of the complexes (longer H–H separation correlates with stronger binding). A key factor is increased back-bonding down the group, as will be discussed below.

Vibrational and Rotational Dynamics of Cr(CO)₃(PCy₃)₂(H₂). Comparison to Mo and W Analogues. Nujol mull IR spectra of Cr(CO)₃(PCy₃)₂(H₂) showed $\nu(\text{CO})$ peaks at 1955 and 1842 cm⁻¹, which did not shift upon D₂ substitution and were similar to those observed¹ for the Mo and W analogues. Two bands clearly associated with the H₂ ligand were located, namely ν_{as} (Cr–H₂) at 1540 cm⁻¹ (w, br) and ν_{s} (Cr–H₂) at 950 cm⁻¹ (m), which shifted to 706 cm⁻¹ for the D₂ isotopomer. These values are similar to those obtained for the W congener, 1568 and 951 cm⁻¹, whereas for the Mo complex ν_{s} (M–H₂) was found at 885 cm⁻¹ (Table 6). Presumably the H–H stretch is obscured by C–H stretches in the 2700–3100-cm⁻¹ region, and $\nu(\text{DD})$ is too weak to be observed or is obscured by $\nu(\text{CO})$. The 400–700-cm⁻¹ region, where deformational modes and metal–carbon stretches occur, shows much more complex patterns and isotopic shifts for

Table 6. IR Frequencies, Rotational Barriers, and Enthalpies of Binding of Group 6 H₂ Complexes

complex	$\nu(\text{HH})^a$	$\nu_{\text{as}}(\text{MH}_2)^a$	$\nu_{\text{s}}(\text{MH}_2)^a$	barrier ^b	$\Delta H_{\text{binding}}^c$
Cr(CO) ₃ (H ₂)	3030	1380	869, 878		
Cr(CO) ₃ (PCy ₃) ₂ (H ₂)		1540	950	1.17(10)	-7.3 ± 0.1
Mo(CO) ₃ (H ₂)	3080				
Mo(CO) ₃ (PCy ₃) ₂ (H ₂)	~2950 ^d	~1420 ^d	885	1.32(10)	-6.5 ± 0.2
Mo(CO)(dppe) ₂ (H ₂)	2650		875	0.7(1)	
W(CO) ₃ (H ₂)	2711		919		
W(CO) ₃ (PCy ₃) ₂ (H ₂)	2690	1568	951	1.9(1)	-9.4 ± 0.9
W(CO) ₃ (PCyPp ₃) ₂ (H ₂) ^e		1565	938		

^a cm⁻¹. In Nujol mulls for phosphine complexes^{5a,26} and liquid Xe¹⁴ or matrices¹³ for the pentacarbonyls. ^b kcal/mol. Values for the PCy₃ complexes are based on H–H distances obtained from solid-state NMR (see text). ^c Enthalpy of H₂ binding, kcal/mol.^{10d} ^d Estimated from observed D₂ isotopomer bands. ^e Cyp = cyclopentyl.²⁶

the Cr–H₂ and D₂ species than had been observed for the IR of the Mo and W analogues. Considerable mixing of $\delta(\text{MCO})$, $\nu(\text{MC})$, and $\delta(\text{MH}_2)$ modes would be expected, and several bands in the Raman and IR spectra of solid W(CO)₃(PCy₃)₂(H₂/D₂) showed small shifts (<20 cm⁻¹; positive and negative) upon deuteration in this region.¹ Similar small shifts have been observed for Cr(CO)₃(H₂/HD/D₂) in matrices¹³ and in liquid xenon solutions¹⁴ for a band in the 650–680-cm⁻¹ region (assigned as the A₁ MCO deformation^{13b}). These shifts could result from a much larger shift of an MH₂ deformational mode (observed or unobserved) to lower frequency for the MD₂ isotopomer. As can be seen in Figure 3, a band at 563 cm⁻¹ is present for the H₂ complex and absent for the D₂ isotopomer, and vice versa for a 527-cm⁻¹ peak. However the small energy difference between these peaks indicates that they represent unrelated modes. The 527-cm⁻¹ band could represent a small positive shift of a band out from beneath non-H₂ related bands at 507 and 486 cm⁻¹. A strong band at 674 cm⁻¹ in the H₂ complex virtually disappears in the D₂ congener (the remaining weaker, sharper band at 677 cm⁻¹ could be due to residual H₂ complex, a ligand mode, or an impurity such as Cr(CO)₄(PCy₃)₂). It is difficult to determine whether this 674-cm⁻¹ band shifts slightly to become one of the closely-spaced bands at 658/638 cm⁻¹ or shifts much further down to become the 527-cm⁻¹ band and hence be an M(H₂) deformational mode. If the latter were true, the isotopic shift ratio of 1.28 would be reasonable; however, the strong intensity of these bands argues against this situation. In any event the data indicate that there are at least two modes in the 400–700-cm⁻¹ region due to η^2 -H₂, as predicted by normal-coordinate analysis.^{1,15}

The determination of an approximate barrier to rotation of the H₂ ligand in Cr(CO)₃(PCy₃)₂(H₂) by inelastic neutron scattering techniques has been previously described.⁴ However, precise measurement of the barrier requires a knowledge of the H–H distance in order to calculate the rotational constant B . Barrier values of 1.3 and 1.5 kcal/mol, respectively, were obtained⁴ for the Cr complex on the basis of H–H distances assumed to be 0.82 and 0.79 Å (those measured for the W and calculated for the Mo analogues). In order to make a self-consistent comparison of the rotational barriers of the present group 6 dihydrogen complexes, we have used the values of $d(\text{HH})$ from the solid-state NMR measurements to recalculate the barrier heights. The reasons for this are that the only complete set of experimental values for the three compounds comes from the solid-state NMR studies

(12) Kubas, G. J.; Burns, C. J.; Eckert, J.; Johnson, S.; Larson, A. C.; Vergamini, P. J.; Unkefer, C. J.; Khalsa, G. R. K.; Jackson, S. A.; Eisenstein, O. *J. Am. Chem. Soc.* **1993**, *115*, 569.

(13) (a) Sweany, R. L. *J. Am. Chem. Soc.* **1985**, *107*, 2374. (b) Sweany, R. L.; Moroz, A. *J. Am. Chem. Soc.* **1989**, *111*, 3577.

(14) Upmacis, R. K.; Poliakov, M.; Turner, J. J. *J. Am. Chem. Soc.* **1986**, *108*, 3645.

(15) Swanson, B. I.; Jones, L. H.; Kubas, G. J. Unpublished results. A preliminary normal coordinate analysis of W(CO)₃(PCy₃)₂(H₂) showed that the force constants for HH and MH stretching were nearly equal. Thus $\nu(\text{HH})$ is a measure of both HH and MH interactions in a way that could only be separated by NCA to extract force constants.

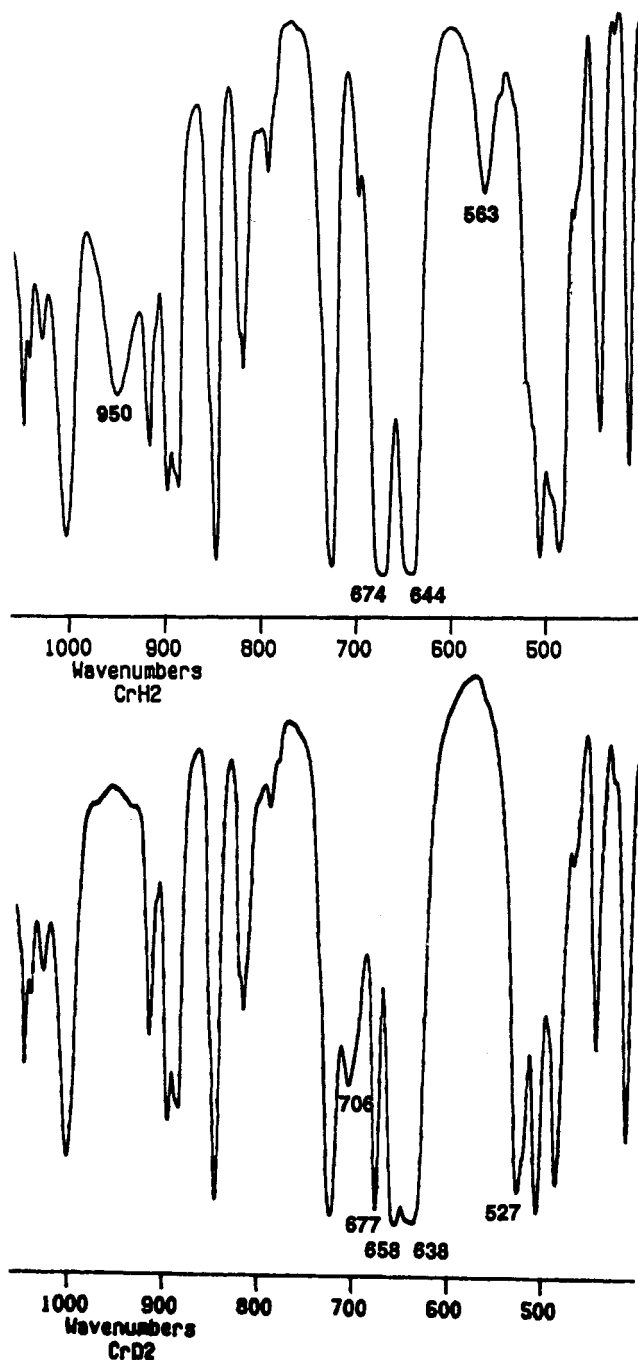


Figure 3. Infrared spectra of $\text{Cr}(\text{CO})_3(\text{PCy}_3)_2(\text{H}_2)$ (upper) and $\text{Cr}(\text{CO})_3(\text{PCy}_3)_2(\text{D}_2)$ (lower) in Nujol mulls.

and that these do not suffer from the very large librational corrections that must be applied to the neutron diffraction results. The resulting values for the 2-fold barrier height are 1.17(10), 1.32(10), and 1.9(1) kcal/mol for the Cr, Mo, and W complexes, respectively. These values are lower than those previously derived¹⁶ because of the larger values of $d(\text{HH})$ obtained from the solid-state NMR results. Uncertainties in the barrier heights are derived from those in the solid-state NMR values for $d(\text{HH})$ and the fit to the rotational tunneling spectra. These calculations are solely based on fitting the rotational tunnel splitting to the V_2 term in the rotational potential. Uncertainty in V_2 is approximately ± 0.05 kcal/mol on the basis of a ± 0.01 -Å uncertainty in $d(\text{HH})$ from NMR and the much smaller uncertainty in the tunneling frequency. The 4-fold term in the

Fourier series expansion of the rotational potential^{16b,c} could not be included in this analysis because experimental data for the higher rotational transitions are not available for the Mo and Cr systems. While this term has been shown to be necessary to obtain a good fit for all the rotational transitions as well as the temperature dependence of the solid-state NMR data, we would expect the relative fraction of V_4 in the rotational potential to be similar for these three isostructural complexes so that the comparison of barrier heights should still be valid.

Correlations of Properties of Group 6 Dihydrogen Complexes. Table 6 summarizes the vibrational data for the Cr, Mo, and W dihydrogen complexes for both $\text{M}(\text{CO})_3(\text{PR}_3)_2$ and low-temperature stable $\text{M}(\text{CO})_5$ fragments, along with rotational barriers and enthalpies of H_2 binding. These results in conjunction with solution stabilities suggest a complicated picture of dihydrogen binding in terms of trends in physical properties down group 6. A major problem for correlating properties of the H_2 complexes is separating $\text{H}_2 \rightarrow \text{M}$ σ -bonding effects from those of $\text{M} \rightarrow \sigma^*$ H_2 back-bonding. The σ interaction is the major contributor to the total $\text{M}-\text{H}_2$ bond interaction¹⁷ and will be discussed first.

Both solution stability and enthalpies of H_2 binding show that Cr binds H_2 significantly more weakly than W, in harmony with general trends³ in bond strength upon going from a first- to a third-row metal. However, an obvious anomaly in Table 6 is the nearly identical symmetric metal- H_2 stretching frequencies in $\text{M}(\text{CO})_3(\text{PCy}_3)_2(\text{H}_2)$ for Cr and W (950 cm^{-1}), whereas the value for Mo is significantly lower. This behavior parallels that for the hydrides $\text{CpM}(\text{CO})_3\text{H}$ where the $\text{M}-\text{H}$ bond dissociation energy favors W over Cr by 11 kcal/mol,¹⁸ yet $\nu(\text{MH})$ values are identical (1828 cm^{-1}) and higher than that for Mo (1809 cm^{-1}).¹⁹ The vibrational data then suggest similar $\text{M}-\text{H}_2$ bond strengths for Cr and W and a lower one for Mo. However the validities of $\nu(\text{MH}_2)$ as a measure of $\text{M}-\text{H}_2$ bond strength and $\nu(\text{HH})$ as an indicator of $\text{H}-\text{H}$ bond activation are questionable because there is considerable mixing in the HH and MH stretching coordinates.¹⁵ Extended Huckel calculations also indicate that Cr and W centers have similar σ -acceptor abilities in model MH_5 fragments.²⁰ Furthermore, the bond dissociation energies of $\text{M}(\text{CO})_5\text{Xe}$ were found to be virtually the same (8–9 kcal/mol) for Cr, Mo, and W within experimental error,²¹ and these should be a pure measure of σ -bonding (back-bonding to Xe cannot occur). Last, $\text{Mo}(\text{CO})_5(\text{H}_2)$ in liquid Xe was reported¹⁴ to have much lower thermal stability than the W or Cr forms and also the highest $\nu(\text{HH})$ (back-bonding to H_2 should again be negligible in these electron-poor species). Summarizing, $\text{H}_2 \rightarrow \text{M}$ σ -bonding strength appears to correlate as $\text{Cr} \sim \text{W} > \text{Mo}$.

In regard to $\text{M} \rightarrow \text{H}_2$ back-bonding, the barrier to H_2 rotation is an excellent *exclusive* measure of this smaller but critical (to H_2 activation) bonding component because $\text{H}_2 \rightarrow \text{M}$ σ -bonding is isotropic about the $\text{M}-\text{H}_2$ axis and cannot contribute to the barrier. It should however be emphasized that the barrier is a relative and not a quantitative measure of back-bonding and depends upon the nature and orientation of the coligands. The values for the barrier to H_2 rotation for the $\text{M}(\text{CO})_3(\text{PCy}_3)_2(\text{H}_2)$ system increase down the group from 1.17 to 1.32 to 1.9 kcal/mol, with that for Mo being closer to that for Cr than to that for W. From this one might conclude that the degree of $\text{H}-\text{H}$ bond activation (weakening by population of $\text{H}_2 \sigma^*$) becomes greater down the group and that $\nu(\text{HH})$ should correspondingly decrease. In this context, it should be recalled that the $\text{H}-\text{H}$ bond of $\text{W}(\text{CO})_3(\text{PCy}_3)_2(\text{H}_2)$ cleaves in solution to give equilibrium amounts of dihydride tautomer,^{2a} while the Cr and Mo congeners

(16) (a) Eckert, J.; Kubas, G. J.; Hall, J. H.; Hay, P. J.; Boyle, C. M. *J. Am. Chem. Soc.* **1990**, *112*, 2324. (b) Eckert, J. *Spectrochim. Acta* **1992**, *48A*, 363. (c) Eckert, J.; Kubas, G. J. *J. Phys. Chem.* **1993**, *97*, 2378.

(17) Hay, P. J. *Chem. Phys. Lett.* **1984**, *103*, 466.

(18) Tilset, M.; Parker, V. D. *J. Am. Chem. Soc.* **1989**, *111*, 6711.

(19) Fritz, H. P. *Adv. Organomet. Chem.* **1964**, *1*, 239.

(20) Jean, Y.; Eisenstein, O.; Volatron, F.; Maouche, B.; Sefta, F. *J. Am. Chem. Soc.* **1986**, *108*, 6587.

(21) Wells, J. R.; Weitz, E. *J. Am. Chem. Soc.* **1992**, *114*, 2783.

do not show this. However, IR spectra of $M(\text{CO})_5(\text{H}_2)$ showed that $\nu(\text{HH})$ decreases in the order $\text{Mo} > \text{Cr} > \text{W}$ (Table 6). Also, the difference in $\nu(\text{HH})$ between $\text{W}(\text{CO})_5(\text{H}_2)$ and $\text{W}(\text{CO})_3(\text{PCy}_3)_2(\text{H}_2)$ would have been expected to be much greater than 21 cm^{-1} because of far superior back-bonding to H_2 in the more electron-rich phosphine complex. Finally, if back-bonding is a factor in the metal- H_2 stretching forces, one would have anticipated $\nu(\text{MH}_2)$ to be significantly higher for W than for Cr, yet a minor ligand change from PCy_3 to tricyclopentylphosphine affected $\nu(\text{MH}_2)$ more than changing the metal (Table 6).

Some of these conflicting IR correlations can be explained by the aforementioned mixing of $\nu(\text{MH}_2)$ and $\nu(\text{HH})$ modes. On the whole, however, it appears that the $\text{M}-\text{H}_2$ σ -interaction is weaker for Mo than for Cr while $\text{M} \rightarrow \text{H}_2$ back-bonding is slightly better for Mo than for Cr in $\text{M}(\text{CO})_3(\text{PR}_3)(\text{H}_2)$. The higher lability of H_2 in $\text{Cr}(\text{CO})_3(\text{PR}_3)(\text{H}_2)$ could be ascribed to this weaker back-bonding, supporting the general belief that back-bonding is much more crucial than σ -bonding in influencing stability, H-H distance, and possibly overall bond strengths. There is some additional evidence for this in the group 8 dihydrogen complexes of the type $\text{MH}(\text{H}_2)\text{P}_4^+$ (P = phosphine donor) where surprisingly the first-row metal Fe gives *more stable* complexes than second-row Ru.^{5c,22,23} Significantly, the rotational barrier

was found to be higher for $[\text{FeH}(\text{H}_2)\text{PP}_3]^+$ (1.82 kcal/mol) than for the Ru congener (1.36 kcal/mol),²³ supporting the contentions that Fe is a better back-bonder than Ru in these systems and that stability of $\text{M}-\text{H}_2$ binding correlates with back-bonding.

In conclusion, much more spectroscopic and structural data need to be generated to fully understand H_2 activation, especially in the area of vibrational modes as a measure of $\text{M}-\text{H}_2$ binding strengths and degree of H-H bond activation. The effects of vibrational and rotational motion of $\eta^2\text{-H}_2$ on the measurement of H-H distances by both crystallographic and NMR methods is also a critical topic for study.

Acknowledgment. We are very grateful to Dr. Carl Hoff of the University of Miami for providing us with generous quantities of $\text{Cr}(\text{CO})_3(\text{naphthalene})$ and $\text{Cr}(\text{CO})_3(\text{PCy}_3)_2$ and for advice on these systems. Work at Los Alamos was supported by the Divisions of Chemical Sciences and Materials Science, Office of Basic Energy Science, U.S. Department of Energy.

Supplementary Material Available: Tables giving the structure determination summary, anisotropic displacement coefficients, fixed H atom coordinates and isotropic displacement coefficients, and complete bond distances and angles (9 pages). Ordering information is given on any current masthead page.

- (22) Bautista, M. T.; Cappellani, E. P.; Drouin, S. D.; Morris, R. H.; Schweitzer, C. T.; Sella, A.; Zubkowski, J. *J. Am. Chem. Soc.* **1991**, *113*, 4876.
(23) Eckert, J.; Albinati, A.; White, R. P.; Bianchini, C.; Peruzzini, M. *Inorg. Chem.* **1992**, *31*, 4241.
(24) Morris, R. H.; Sawyer, J. F.; Shiralian, M.; Zubkowski, J. D. *J. Am. Chem. Soc.* **1985**, *107*, 5581.
(25) Ricci, J. S.; Koetzle, T. F.; Bautista, M. T.; Hofstede, T. M.; Morris, R. H.; Sawyer, J. F. *J. Am. Chem. Soc.* **1989**, *111*, 8823.

- (26) Khalsa, G. R. K.; Kubas, G. J.; Unkefer, C. J.; Van Der Sluys, L. S.; Kubat-Martin, K. A. *J. Am. Chem. Soc.* **1990**, *112*, 3855.
(27) Litster, S. J.; Redhouse, A. D.; Simpson, S. J. *Proceedings of the Conference on Chemistry of the Platinum Metals*; Cambridge University: Cambridge, U.K., 1990; Abstract C-48.
(28) Conroy-Lewis, F. M.; Simpson, S. J. *J. Chem. Soc., Chem. Commun.* **1987**, 1675.
(29) Chinn, M. S.; Heinekey, D. M. *J. Am. Chem. Soc.* **1987**, *109*, 5865.